

Stationary Solitons in discrete NLS with non-nearest neighbour interactions

Vassilis M. Rothos[§], Stavros Anastassiou[†] and Katerina G. Hadjifotinou[‡]

[§] *Department of Mechanical Engineering, Faculty of Engineering, Aristotle University of Thessaloniki, Thessaloniki 54124, Greece*

[†] *Department of Mathematics, University of West Macedonia, Kastoria 52100, Greece*

[‡] *Department of Mathematics, Faculty of Science, Aristotle University of Thessaloniki, Thessaloniki 54124, Greece*

July 23, 2024

Abstract

The aim of this paper is to provide a construction of stationary discrete solitons in an extended one-dimensional Discrete NLS model with non-nearest neighbour interactions. These models, models of the type with long-range interactions were studied in various other contexts. In particular, it was shown that, if the interaction strength decays sufficiently slowly as a function of distance, it gives rise to bistability of solitons, which may find applications in their controllable switching. Dynamical lattices with long-range interactions also serve as models for energy and charge transport in biological molecules. Using a dynamical systems method we are able to construct, with great accuracy, stationary discrete solitons for our model, for a large region of the parameter space.

Keywords: discrete NLS equation, solitons, invariant manifolds, parametrization method
MSC2010: 35Q53, 35B08, 37G20, 35A35

1 Introduction

Among the most prominent differential equations in applied mathematics are nonlinear Schrödinger (NLS) equations, a class of partial differential equations which have been employed as models in diverse branches of physics. The nonlinear Schrödinger (NLS) equation describes a very large variety of physical systems since it is the lowest order nonlinear (cubic) partial differential equation that describes the propagation of modulated waves. For example, two of the most salient applications of NLS equations, that will be the main theme of this session, stem from the realm on nonlinear optics and Bose-Einstein condensates (BECs). In optics, the NLS stems from the nonlinear (Kerr) response of the refractive index of some nonlinear media. On the other hand, for BECs, the mean-field description of a condensed cloud of atoms is well approximate, at low enough temperatures, by the NLS with an external potential.

It is well known that the solitons described by the regular NLS equations with power-law nonlinearities may be unstable if the number of space dimensions or (and) the power of nonlinearity is sufficiently high [5], [6]. In some cases the instabilities result in the collapse (blowup) which occurs at finite time (in two space dimensions this is the so-called self-focusing). In many papers, the main

attention in the studies of stabilizations of instabilities has been paid to the saturation of nonlinearity. On the other hand, the effects of higher-order dispersion may also play a significant role [11]. In this work, we continue the investigation of the stabilizing role of higher-order dispersive effects using a comparatively simple model described by the equation

$$i\partial_t\Psi + \frac{1}{2}\Delta\Psi + \frac{1}{2}\gamma\Delta^2\Psi + |\Psi|^{2p}\Psi = 0, \quad (1)$$

where p is an integer number, and

$$p \geq 1, \quad \Delta = \nabla_\alpha \nabla_\alpha, \quad \alpha = 1, \dots, D, \quad D = 1, 2, 3$$

(summation over repeated indices is assumed; D is the number of space dimensions). The term containing Δ^2 describes the higher-order dispersion. Eq. (1) permits one to investigate the role of space dimensions, strength of nonlinearity and higher-order dispersion effects in the soliton stabilization. The criteria for soliton stability, briefly reported earlier [11], contain D and p not separately, but through the product Dp ; at $\gamma = 0$ they turn into the conditions derived for the NLS type equations with the lowest order dispersion [5], [6]. Fourth-order Schrödinger equations have been introduced to take into account the role of small fourth-order dispersion terms in the propagation of intense laser beams in a bulk medium with Kerr nonlinearity. Such fourth-order Schrödinger equations have been studied from the mathematical viewpoint in Fibich, Ilan and Papanicolaou [20] who describe various properties of the equation in the subcritical regime, with part of their analysis relying on very interesting numerical developments.

During the early years, studies of intrinsic localized modes were mostly of a mathematical nature, but the ideas of localized modes soon spread to theoretical models of many different physical systems, and the discrete breather concept has been recently applied to experiments in several different physics subdisciplines. Most nonlinear lattice systems are not integrable even if the partial differential equation (PDE) model in the continuum limit is. While for many years spatially continuous nonlinear PDE's and their localized solutions have received a great deal of attention, there has been increasing interest in spatially discrete nonlinear systems. Namely, the dynamical properties of nonlinear systems based on the interplay between discreteness, nonlinearity and dispersion (or diffraction) can find wide applications in various physical, biological and technological problems. Examples are coupled optical fibres (self-trapping of light) [4, 9, 13, 14], arrays of coupled Josephson junctions [8], nonlinear charge and excitation transport in biological macromolecules, charge transport in organic semiconductors [2].

Prototype models for such nonlinear lattices take the form of various nonlinear lattices [10], a particularly important class of solutions of which are the so called discrete breathers which are homoclinic in space and oscillatory in time. Other questions involve the existence and propagation of topological defects or kinks which mathematically are heteroclinic connections between a ground and an excited steady state. Prototype models here are discrete version of sine-Gordon equations, also known as Frenkel-Kontorova (FK) models, e.g. [22]. There are many outstanding issues for such systems relating to the global existence and dynamics of localized modes for general nonlinearities, away from either continuum or anti-continuum limits.

In the main part of the previous studies of the discrete NLS models the dispersive interaction was assumed to be short-ranged and a nearest-neighbour approximation was used. However, there exist physical situations that definitely can not be described in the framework of this approximation.

The existence of localized traveling waves (sometimes called “moving discrete breathers” or “discrete solitons”) in discrete nonlinear Schrödinger (DNLS) lattices has shown itself to be a delicate question of fundamental scientific interest (see e.g [16]). This interest is largely due to the experimental realization of solitons in discrete media, such as waveguide arrays [23] optically induced photorefractive crystals [24] and Bose-Einstein condensates coupled to an optical lattice trap [18].

The prototypical equation that emerges to explain the experimental observations is the DNLS model of the form:

$$i\ddot{u}_n(t) = \frac{u_{n+1}(t) - 2u_n(t) + u_{n-1}(t)}{h^2} + F(u_{n+1}(t), u_n(t), u_{n-1}(t)), \quad (2)$$

where the integer $n \in \mathbb{Z}$ labels a one-dimensional array of lattice sites, with spacing h . Alternatively h can be thought of as representing the inverse coupling strength between adjacent sites. The nonlinear term F can take a number of different forms:

- DNLS equation: $F_{\text{DNLS}} = |u_n|^2 u_n$,
- Abolowitz-Ladik (AL) model [1]: $F_{\text{AL}} = |u_n|^2 (u_{n+1} + u_{n-1})$,
- Salerno model [7]: $F_{\text{S}} = 2(1 - \alpha)F_{\text{DNLS}} + \alpha F_{\text{AL}}$,
- cubic-quintic DNLS: $F_{3-5} = (|u_n|^2 + \alpha|u_n|^4)u_n$,
- saturable DNLS: $F_{\text{sat}} = \frac{u_n}{1+|u_n|^2}$,
- generalised cubic DNLS equation:

$$\begin{aligned} F_{g3} = & \alpha_1 |u_n|^2 u_n + \alpha_2 |u_n|^2 (u_{n+1} + u_{n-1}) + \alpha_3 u_n^2 (\bar{u}_{n+1} + \bar{u}_{n-1}) \\ & \alpha_4 (|u_{n+1}|^2 + |u_{n-1}|^2) u_n + \alpha_5 (\bar{u}_{n+1} u_{n-1} + u_{n+1} \bar{u}_{n-1}) u_n + \\ & \alpha_6 (u_{n+1}^2 + u_{n-1}^2) \bar{u}_n + \alpha_7 u_{n+1} u_{n-1} \bar{u}_n \\ & + \alpha_8 (|u_{n+1}|^2 u_{n+1} + |u_{n-1}|^2 u_{n-1}) + \alpha_9 (u_{n+1}^2 \bar{u}_{n-1} + u_{n-1}^2 \bar{u}_{n+1}) \\ & + \alpha_{10} (|u_{n+1}|^2 u_{n-1} + |u_{n-1}|^2 u_{n+1}). \end{aligned} \quad (3)$$

where $\bar{\cdot}$ is used to represent complex conjugation.

Note that when $\alpha_1 = 2(1 - \alpha_2)$, $\alpha_2 \in \mathbb{R}$, and $\alpha_j = 0$ for $3 \leq j \leq 10$, the nonlinear function F_{g3} reduces to the Salerno nonlinearity F_{S} . Stationary localized solutions to (2) of the form $u(n, t) = e^{-i\omega t} U(n)$ abound in such models under quite general hypotheses on the function F , and indeed one can pass to the continuum limit $h \rightarrow 0$, $x = nh$ and find the corresponding solutions to continuum NLS equations of the form

$$i\dot{u}_n(t) = u_{xx} + f(|u|^2)u. \quad (4)$$

The goal of this work is to study the existence of special solutions (stationary solutions) for extended nonlinear lattice models of the 4th order NLS-type equation (1).

We consider the DNLS-type model with the next-nearest-neighbor interaction for simplicity of our analysis (we could consider the direct discretization of (1), in a future publication)

$$i\ddot{u}_n + |u_n|^2 u_n + \epsilon (u_{n+1} - 2u_n + u_{n-1} + A(u_{n+2} + u_{n-2})) = 0, \quad (5)$$

where $u_n : \mathbb{R}_+ \rightarrow \mathbb{C}$, $n \in \mathbb{Z}$, $\epsilon > 0$.

We seek steady-state solutions of this equation, i.e. solutions that satisfy $\dot{u}_n(t) = 0, \forall n \in \mathbb{Z}$.

We begin our study in section 2, where we set $A = 0$ in equation (5). A two-dimensional mapping is obtained and its qualitative behaviour is studied, which turns out to be quite simple.

In section 3, we turn our attention to the case where $A \neq 0$. In this case, by setting $\dot{u}_n(t) = 0, \forall n \in \mathbb{Z}$, a four-dimensional mapping is obtained, the qualitative properties of which are of interest here. Its symmetry properties are analysed and the stability of its fixed points is determined. We then proceed to compute orbits homoclinic to the origin for this, four-dimensional, mapping. To achieve that, we employ the Parametrization Method and are able to locate, with great accuracy, homoclinic points when parameters A , ϵ belong to a certain region of the parameter space. We also argue that these homoclinic points are transverse, implying the existence of complicated behaviour in the phase space of our mapping. Note that, in this way, we have constructed stationary soliton solutions of equation (5). Last section contains the conclusions of this work.

2 The 2–d mapping

To study steady–state solutions for equation (5), we let $\dot{u}_n = 0$. We begin, in this section, by setting $A = 0$. We get:

$$|u_n|^2 u_n + \epsilon(u_{n+1} - 2u_n + u_{n-1}) = 0 \Rightarrow u_{n+1} = -u_{n-1} + 2u_n - \frac{1}{\epsilon}|u_n|^2 u_n.$$

By introducing variables $x = u_{n-1}$, $y = u_n$, we arrive at the following mapping of the complex plane:

$$f_0 : \mathbb{C}^2 \rightarrow \mathbb{C}^2, \quad f_0(x, y) = (y, -x + 2y - \frac{1}{\epsilon}|y|^2 y). \quad (6)$$

Observe that $f_0(x, y) \in \mathbb{R}^2$ if, and only if, $(x, y) \in \mathbb{R}^2$. We therefore restrict our attention to the case where the variables are real, and consider the following mapping, which we also denote by f_0 :

$$f_0 : \mathbb{R}^2 \rightarrow \mathbb{R}^2, \quad f_0(x, y) = (y, -x + 2y - \frac{1}{\epsilon}y^3). \quad (7)$$

In this section, it is our intention to study mapping (7).

Observe that it is a generalised Hénon map, i.e., a mapping of the form:

$$(x, y) \mapsto (y, \delta x + p(y)),$$

which has been extensively studied, not only in its two–dimensional form presented above, but in its higher dimensional analogues as well (see, for example, [12, 15, 17, 26, 29, 30, 31, 36, 37, 40, 42] and references therein).

The reader can easily confirm that, $\forall (x, y) \in \mathbb{R}^2$, $|Df_0(x, y)| = 1$, thus our mapping is area–preserving, while its inverse is given by:

$$f_0^{-1} : \mathbb{R}^2 \rightarrow \mathbb{R}^2, \quad f_0^{-1}(x, y) = (2x - \frac{1}{\epsilon}x^3 - y, x).$$

Moreover, mapping f_0 is symmetric with respect to the involution $\sigma_1(x, y) = (-x, -y)$, i.e. relation $f_0 \circ \sigma_1 = \sigma_1 \circ f_0$ holds, while it is reversible with respect to the involutions $\sigma_2(x, y) = (y, x)$, $\sigma_3(x, y) = (-y, -x)$, that is,

$$f_0 \circ \sigma_2 = \sigma_2 \circ f_0^{-1}, \quad f_0 \circ \sigma_3 = \sigma_3 \circ f_0^{-1}.$$

Let us locate bounded orbits for mapping (7).

2.1 Proposition *Mapping (7) possesses, $\forall \epsilon \in \mathbb{R}$, a unique fixed point, located at the origin, which is a degenerate parabolic point. This fixed point is stable if, and only if, $\epsilon > 0$. The non–wandering set of the mapping is contained in $[-2\sqrt{|\epsilon|}, 2\sqrt{|\epsilon|}] \times [-2\sqrt{|\epsilon|}, 2\sqrt{|\epsilon|}] \subset \mathbb{R}^2$.*

Proof. Simple calculations show that, indeed, the origin is the unique fixed point of mapping f_0 , having a double eigenvalue equal to 1.

Consider the change of variables $\psi(x, y) = (x + y, 2x + y)$. It is area–preserving and satisfies relation $f_0 \circ \psi = \psi \circ T$, where:

$$T(x, y) = (x - \frac{1}{\epsilon}(2x + y)^3, x + y + \frac{1}{\epsilon}(2x + y)^3).$$

As shown in [3], the origin is a stable fixed point for mapping T if, and only if, $-\frac{1}{\epsilon} < 0$; thus ϵ should be positive.

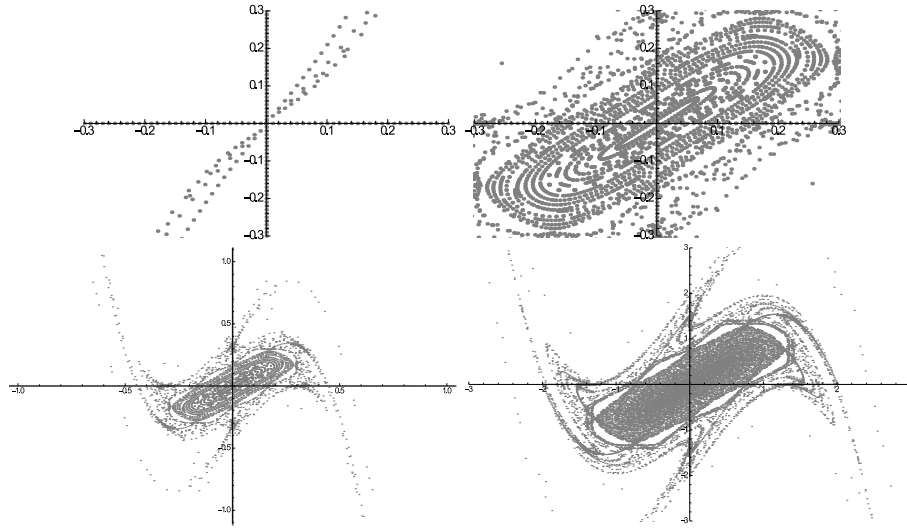


Figure 1: Phase portraits for mapping (7). First row, left: $\epsilon = -0.1$ and all orbits, except from the fixed point, tend to infinity. First row, right: $\epsilon = 0.1$ and the origin is a stable fixed point. Second row, left: $\epsilon = 0.1$ global phase portrait. Second row, right: $\epsilon = 2$ global phase portrait. The same initial conditions were used, for all four portraits.

To locate the non-wandering set of mapping (7), we employ the results of [25]. We adopt the notation used there, and rewrite our mapping as a difference equation with respect to the variable x :

$$\frac{1}{\epsilon}x_{n+1}^3 + x_n - 2x_{n+1} + x_{n+2} = 0.$$

The leading term is $\frac{1}{\epsilon}x_{n+1}^3$, while the roots of polynomial $|\frac{1}{\epsilon}|x^3 - 4x$ are 0 and $\pm 2\sqrt{|\epsilon|}$, thus the first coordinate of every point of the non-wandering set of (7) belongs to $[-2\sqrt{|\epsilon|}, 2\sqrt{|\epsilon|}]$. The second coordinate can be treated in exactly the same way. \square

In figure (1) we present the phase portrait of mapping (7), for specific values of the parameter ϵ . We observe that, for $\epsilon < 0$, all orbits, with the exception of the fixed point, tend to infinity, while for $\epsilon > 0$, the origin is a stable fixed point. For different, positive, values of ϵ , the structure of the phase portrait presents no qualitative change.

We shall now turn our attention to the case where $A \neq 0$, in equation (5).

3 The 4-d mapping

Seeking steady-state solutions of equation (5), we set $\dot{u}_n = 0$ and $u_{n-2} = x, u_{n-1} = y, u_n = z, u_{n+1} = w$. We thus define the mapping:

$$f : \mathbb{C}^4 \rightarrow \mathbb{C}^4, f(x, y, z, w) = (y, z, w, -\frac{1}{\epsilon A}|z|^2z - \frac{1}{A}w + \frac{2}{A}z - \frac{1}{A}y - x).$$

Observe that, as above, $f(x, y, z, w) \in \mathbb{R}^4$ if, and only if, $(x, y, z, w) \in \mathbb{R}^4$. We therefore restrict our attention to:

$$f : \mathbb{R}^4 \rightarrow \mathbb{R}^4, f(x, y, z, w) = (y, z, w, -x - \frac{1}{A}y + \frac{2}{A}z - \frac{1}{\epsilon A}z^3 - \frac{1}{A}w). \quad (8)$$

It is this mapping that we wish to study, in this section.

This mapping is volume-preserving, since $|Df(x, y, z, w)| = 1$, $\forall(x, y, z, w) \in \mathbb{R}^4$. Moreover, its inverse is also polynomial:

$$f^{-1} : \mathbb{R}^4 \rightarrow \mathbb{R}^4, \quad f^{-1}(x, y, z, w) = (-w - \frac{1}{A}x + \frac{2}{A}y - \frac{1}{\epsilon A}y^3 - \frac{1}{A}z, x, y, z).$$

As in the 2-d case, the following relations hold:

$$(a) f \circ \sigma_4 = \sigma_4 \circ f, \quad (b) f \circ \sigma_5 = \sigma_5 \circ f^{-1}, \quad (c) f \circ \sigma_6 = \sigma_6 \circ f^{-1} \quad (9)$$

where:

$$\begin{aligned} \sigma_4(x, y, z, w) &= (-x, -y, -z, -w), \quad \sigma_5(x, y, z, w) = (w, z, y, x), \\ \sigma_6(x, y, z, w) &= (-w, -z, -y, -x). \end{aligned}$$

We locate the non-wandering set of mapping (8) as follows:

3.1 Proposition *The non-wandering set of mapping (8) is contained in*

$$\left[-\sqrt{|\epsilon A|(2 + \frac{4}{|A|})}, \sqrt{|\epsilon A|(2 + \frac{4}{|A|})} \right]^4 \subset \mathbb{R}^4.$$

Proof. The result follows from [25]. We rewrite mapping (8) as a difference equation, with respect to x :

$$\frac{1}{\epsilon A}x_{n+2}^3 + x_n + \frac{1}{A}x_{n+1} - \frac{2}{A}x_{n+2} + \frac{1}{A}x_{n+3} + x_{n+4} = 0.$$

The leading term is $\frac{1}{\epsilon A}x_{n+2}^3$, while the roots of polynomial $|\frac{1}{\epsilon A}|x^3 - (2 + \frac{4}{|A|})x$ are $0, \pm\sqrt{|\epsilon A|(2 + \frac{4}{|A|})}$, thus the projection of the non-wandering set in the first axis is contained in $\left[-\sqrt{|\epsilon A|(2 + \frac{4}{|A|})}, \sqrt{|\epsilon A|(2 + \frac{4}{|A|})} \right]$.

The inclusions concerning the projections on the other axes are proved in the same way. \square

Let us now proceed to study the mappings fixed points.

3.1 Fixed points and their stability

In general, mapping f possesses three fixed points, namely:

$$(0, 0, 0, 0), \quad (\pm\sqrt{-2\epsilon A}, \pm\sqrt{-2\epsilon A}, \pm\sqrt{-2\epsilon A}, \pm\sqrt{-2\epsilon A}).$$

To study their stability, we shall use the following:

3.1 Lemma Polynomial $p(x) = x^4 + ax^3 + bx^2 + ax + 1$, where $a, b \in \mathbb{R}$, possesses four real roots if, and only if, one of the following conditions is satisfied.

1. $b < -2$ and $-\frac{1}{2}\sqrt{4 + 4b + b^2} < a < \frac{1}{2}\sqrt{4 + 4b + b^2}$.
2. $b > 6$ and $-\frac{1}{2}\sqrt{4 + 4b + b^2} < a < -\sqrt{-8 + 4b}$.
3. $b > 6$ and $\sqrt{-8 + 4b} < a < \frac{1}{2}\sqrt{4 + 4b + b^2}$.

These roots are of the form $\lambda_1, \lambda_1^{-1}, \lambda_2, \lambda_2^{-1}$, where $\lambda_1, \lambda_2 \in (0, 1)$.

Proof. To determine for which values of a, b , $p(x)$ possesses real roots, we shall employ the Sturm theorem (see [28]).

We construct the Sturm polynomials for $p(x)$, as follows:

$$\begin{aligned} p_0(x) &= p(x) = x^4 + ax^3 + bx^2 + ax + 1 \\ p_1(x) &= p'(x) = a + 2bx + 3ax^2 + 4x^3 \\ p_2(x) &= -1 + \frac{a^2}{16} + \left(\frac{ab}{8} - \frac{3a}{4}\right)x + \left(\frac{3a^2}{16} - \frac{b}{2}\right)x^2 \\ p_3(x) &= -\frac{16(8 + a^2 - 4b)(a(6 - b) + 6a^2x - 2b(2 + b)x)}{(3a^2 - 8b)^2} \\ p_4(x) &= -\frac{(3a^2 - 8b)^2(4a^2 - (2 + b)^2)}{64(-3a^2 + b(2 + b))^2}. \end{aligned}$$

We remind that, as dictated by Sturm's theorem, $p_i(x)$, $i \geq 2$, is defined to be the remainder of the division of $p_{i-2}(x)$ by $p_{i-1}(x)$, with its sign changed.

In order for $p(x)$ to possess 4 real roots, it is sufficient and necessary to have:

$$\frac{3a^2}{16} - \frac{b}{2} > 0, \quad (8 + a^2 - 4b)(6a^2 - 2b(2 + b)) < 0, \quad (2 + b)^2 - 4a^2 > 0,$$

from which inequalities we deduce the conditions given in the statement of the lemma.

To prove that these roots are of the form claimed above, note that mapping:

$$s \mapsto \frac{1 + s}{1 - s},$$

maps the left, open, half-plane of \mathbb{C} to the closed unit disk. In the s -variable, polynomial $p(x)$ takes the following form (after multiplication with $(1 - s)^4$):

$$2 + 2a + b - 2(-6 + b)s^2 + (2 - 2a + b)s^4.$$

The Routh–Hurwitz criterion (see [19]), ensures that the roots of this polynomial appear in pairs and that members of the same pair are of equal norm, but opposite sign. Mapping $s \mapsto \frac{1+s}{1-s}$ maps such pairs to pairs of the form λ, λ^{-1} . \square

We are now able to state results concerning the stability of fixed points mapping (8) possesses.

3.2 Corollary

1. The origin is always a fixed point for mapping (8). Its eigenvalues are:

- two pairs of complex-conjugate numbers, for $A \in (-\infty < \frac{-2+\sqrt{2}}{4}) \cup (2, +\infty)$
- all real, for $A \in [\frac{-2+\sqrt{2}}{4}, 0)$.
- two real and a pair of complex-conjugate eigenvalues, for $A \in (0, 2]$.

2. For $\epsilon A < 0$, mapping f possesses two more fixed points, symmetric to each other, namely $(\pm\sqrt{-2\epsilon A}, \pm\sqrt{-2\epsilon A}, \pm\sqrt{-2\epsilon A}, \pm\sqrt{-2\epsilon A})$. Their eigenvalues are:

- two real and a pair of complex-conjugate numbers, for $A \in (-1, 0)$.
- all real, for $A \in (-\infty, -1] \cup (0, +\infty)$.

3. In any case, the eigenvalues are necessarily of the form $\lambda_1, \lambda_1^{-1}, \lambda_2, \lambda_2^{-1}$.

Proof.

1. The characteristic polynomial of f at the origin is:

$$k_0(x) = x^4 + \frac{1}{A}x^3 - \frac{2}{A}x^2 + \frac{1}{A}x + 1.$$

It is obtained from polynomial $p(x)$, of the previous lemma, for $a = \frac{1}{A}$ and $b = -\frac{2}{A}$, thus the conclusion. The discriminant of this polynomial equals

$$\frac{4(-2 - 31A - 144A^2 - 176A^3 + 64A^5)}{A^5}.$$

The conclusions follow from the lemma above and the properties of discriminants of polynomials (see [28]).

2. The characteristic polynomial of f at the non-trivial fixed points is:

$$k_1(x) = x^4 + \frac{1}{A}x^3 - (6 + \frac{2}{A})x^2 + \frac{1}{A}x + 1.$$

It is obtained from the polynomial $p(x)$ of the lemma above, for $a = \frac{1}{A}$, $b = -(6 + \frac{2}{A})$. Its discriminant equals:

$$\frac{16(1 + 17A + 144A^2 + 640A^3 + 1536A^4 + 1024A^5)}{A^5}.$$

Hence the conclusion. □

Since our main intention is to steady-state solitons for equation (5), we turn our attention to orbits homoclinic to the origin, for mapping (8).

3.2 Homoclinics to the origin

To locate solutions homoclinic to the origin, we restrict our attention to the case where all eigenvalues are real. Thus, according to the results presented above, we let $A \in [\frac{-2+\sqrt{2}}{4}, 0)$. We also let $\epsilon \in [-1, 1]$ and, in view of section 2, we expect that homoclinics should exist for positive values of ϵ .

For these parameter values, the origin is a saddle point for mapping (8). It is easy to verify that ± 1 are not eigenvalues of $Jf(0, 0, 0, 0)$; thus the Jacobian matrix possesses two eigenvalues of absolute value less than 1, which we shall denote by λ_1, λ_2 , and two eigenvalues of absolute values greater than 1, which we shall denote by $\lambda_3 = \lambda_1^{-1}, \lambda_4 = \lambda_2^{-1}$.

The origin is therefore a hyperbolic saddle, having a two-dimensional stable and a two-dimensional unstable manifold, denoted by $W^s(O), W^u(O)$ respectively. It is our purpose here to determine if these two manifolds intersect.

To achieve that, we employ the Parametrization Method. We shall briefly sketch this method here, as applied in our case, however the interested reader should consult [41, 38, 39, 33, 34, 32] for applications of this method to the study of maps and [35] for many more applications.

Manifolds $W^s(O), W^u(O)$ are analytic, according to the Stable Manifold Theorem (see, for example, [19]) and can therefore be represented, at least locally, using analytic mappings. That is, the stable and the unstable manifolds can be thought of as the images of mappings $S^s, S^u : \mathbb{R}^2 \rightarrow \mathbb{R}^4$, respectively.

Restricted on the stable (unstable) manifold, mapping (8) acts as a contraction (dilation), with contraction (dilation) rates λ_1, λ_2 (λ_3, λ_4). Therefore, one gets the following equations:

$$f \circ S^s(u, v) = S^s(\lambda_1 u, \lambda_2 v) \quad (10)$$

$$f \circ S^u(u, v) = S^u(\lambda_3 u, \lambda_4 v). \quad (11)$$

The symmetry properties (9) of mapping (8) are reflected on these two manifolds. Indeed, note that:

$$\begin{aligned} f \circ S^s(u, v) &= S^s(\lambda_1 u, \lambda_2 v) \Rightarrow \\ \Rightarrow \sigma_4 \circ f \circ S^s(u, v) &= \sigma_4 \circ S^s(\lambda_1 u, \lambda_2 v) \Rightarrow \\ \xrightarrow{9(a)} f \circ \sigma_4 \circ S^s(u, v) &= \sigma_4 \circ S^s(\lambda_1 u, \lambda_2 v), \end{aligned}$$

meaning that $\sigma_4 \circ S^s$ is also a stable manifold of the origin. Thus, the image of S^s is symmetric, with respect to σ_4 . The same holds for the image of S^u .

Note also that:

$$\begin{aligned} f \circ S^s(u, v) &= S^s(\lambda_1 u, \lambda_2 v) \Rightarrow \\ \Rightarrow \sigma_5 \circ f \circ S^s(u, v) &= \sigma_5 \circ S^s(\lambda_1 u, \lambda_2 v) \Rightarrow \\ \xrightarrow{9(b)} f^{-1} \circ \sigma_5 \circ S^s(u, v) &= \sigma_5 \circ S^s(\lambda_1 u, \lambda_2 v), \end{aligned}$$

Thus, $\sigma_5 \circ S^s$ is a stable manifold for f^{-1} and therefore an unstable manifold for f ; that is, S^u is the image of S^s under the symmetry σ_5 and the same of course holds for symmetry σ_6 .

We begin by computing the stable manifold of the origin. Since this manifold is analytic, it can be represented as a, convergent, power series:

$$S^s : \mathbb{R}^2 \rightarrow \mathbb{R}^4, \quad S^s(u, v) = \begin{bmatrix} \sum_{n=0}^{+\infty} \sum_{m=0}^{+\infty} a_1^{nm} u^n v^m \\ \sum_{n=0}^{+\infty} \sum_{m=0}^{+\infty} a_2^{nm} u^n v^m \\ \sum_{n=0}^{+\infty} \sum_{m=0}^{+\infty} a_3^{nm} u^n v^m \\ \sum_{n=0}^{+\infty} \sum_{m=0}^{+\infty} a_4^{nm} u^n v^m \end{bmatrix}.$$

In the notation above, a_i^{nm} , $i = 1, \dots, 4$, stands for the i -th coefficient of order $n + m$; that is, the exponent is not a power.

The left-hand side of equation (10) reads as:

$$\left[\begin{array}{c} \sum_{n=0}^{+\infty} \sum_{m=0}^{+\infty} a_2^{nm} u^n v^m \\ \sum_{n=0}^{+\infty} \sum_{m=0}^{+\infty} a_3^{nm} u^n v^m \\ \sum_{n=0}^{+\infty} \sum_{m=0}^{+\infty} a_4^{nm} u^n v^m \\ - \sum_{n=0}^{+\infty} \sum_{m=0}^{+\infty} a_1^{nm} u^n v^m - \frac{1}{A} \sum_{n=0}^{+\infty} \sum_{m=0}^{+\infty} a_2^{nm} u^n v^m + \frac{2}{A} \sum_{n=0}^{+\infty} \sum_{m=0}^{+\infty} a_3^{nm} u^n v^m - \\ - \frac{1}{\epsilon A} \left(\sum_{n=0}^{+\infty} \sum_{m=0}^{+\infty} a_3^{nm} u^n v^m \right)^3 - \frac{1}{A} \sum_{n=0}^{+\infty} \sum_{m=0}^{+\infty} a_4^{nm} u^n v^m \end{array} \right],$$

while the right-hand side equals:

$$\begin{bmatrix} \sum_{n=0}^{+\infty} \sum_{m=0}^{+\infty} \lambda_1^n \lambda_2^m a_1^{nm} u^n v^m \\ \sum_{n=0}^{+\infty} \sum_{m=0}^{+\infty} \lambda_1^n \lambda_2^m a_2^{nm} u^n v^m \\ \sum_{n=0}^{+\infty} \sum_{m=0}^{+\infty} \lambda_1^n \lambda_2^m a_3^{nm} u^n v^m \\ \sum_{n=0}^{+\infty} \sum_{m=0}^{+\infty} \lambda_1^n \lambda_2^m a_4^{nm} u^n v^m \end{bmatrix}.$$

Since:

$$\left(\sum_{n=0}^{+\infty} \sum_{m=0}^{+\infty} a_3^{nm} u^n v^m \right)^3 = \sum_{n=0}^{+\infty} \sum_{m=0}^{+\infty} \sum_{i=0}^n \sum_{j=0}^m \sum_{k=0}^i \sum_{l=0}^j a_3^{n-i, m-j} a_3^{i-k, j-l} a_3^{k, l} u^n v^m,$$

by equating terms of the same degree, we arrive at the following system:

$$\begin{aligned} -\lambda_1^n \lambda_2^m a_1^{nm} + a_2^{nm} &= 0 \\ -\lambda_1^n \lambda_2^m a_2^{nm} + a_3^{nm} &= 0 \\ -\lambda_1^n \lambda_2^m a_3^{nm} + a_4^{nm} &= 0 \\ -a_1^{nm} - \frac{1}{A} a_2^{nm} + \frac{2}{A} a_3^{nm} - \left(\frac{1}{A} + \lambda_1^n \lambda_2^m \right) a_4^{nm} &= \\ = \frac{1}{\epsilon A} \sum_{i=0}^n \sum_{j=0}^m \sum_{k=0}^i \sum_{l=0}^j a_3^{n-i, m-j} a_3^{i-k, j-l} a_3^{k, l} & \end{aligned} \quad (12)$$

Note that system (12) is a linear system, with respect to the unknowns a_i^{nm} , $i = 1, \dots, 4$. It can be used to find the coefficients of parametrization S^s of arbitrary, finite, order, as long as the lower-order coefficients are known and the eigenvalues λ_i , $i = 1, 2$ satisfy a non-resonance condition.

For example, for $n = m = 0$, system (12) becomes:

$$\begin{aligned} -a_1^{00} + a_2^{00} &= 0 \\ -a_2^{00} + a_3^{00} &= 0 \\ -a_3^{00} + a_4^{00} &= 0 \\ -a_1^{00} - \frac{1}{A} a_2^{00} + \frac{2}{A} a_3^{00} - \frac{1}{A} a_4^{00} &= 0 \end{aligned}$$

from which we conclude that $a_i^{00} = 0$, $i = 1, \dots, 4$. This reflects the fact that the stable manifold of the origin contains the origin; thus parametrization S^s should satisfy $S^s(0, 0) = (0, 0, 0, 0)$.

Similarly, for $n = 1, m = 0$ and $n = 0, m = 1$ we get:

$$(a_1^{10}, a_2^{10}, a_3^{10}, a_4^{10}) = w_1, \quad (a_1^{01}, a_2^{01}, a_3^{01}, a_4^{01}) = w_2,$$

where w_1, w_2 are the eigenvectors corresponding to the eigenvalues λ_1, λ_2 . This reflects the fact that the tangent space at the origin of the stable manifold should be the stable eigenspace of the origin, i.e., $T_0(\text{Im}(S^s)) = E^s(0)$ and therefore:

$$\frac{\partial S^s}{\partial u}(0, 0) = w_1, \quad \frac{\partial S^s}{\partial v}(0, 0) = w_2.$$

The low-order terms are therefore known and one can proceed to the computation of higher-order terms, using system (12), recursively.

The unstable manifold S^u can be computed in exactly the same way, the only difference being that eigenvalues λ_1, λ_2 should be replaced with the unstable ones λ_3, λ_4 .

Since, however, the coefficients of both the stable and the unstable manifold can be computed to a finite order, we end up with a polynomial approximation $P^s(u, v)$ for the stable manifold $S^s(u, v)$ and a polynomial approximation $P^u(u, v)$ of the unstable manifold $S^u(u, v)$.

To locate homoclinic points, one should solve equation:

$$P^u(u_1, v_1) = P^s(u_2, v_2). \quad (13)$$

Solutions (u_1, v_1, u_2, v_2) correspond to homoclinic points of mapping (8). These points can be represented both as $P^u(u_1, v_1)$ and as $P^s(u_2, v_2)$.

We intend to solve equation (13) numerically. Therefore, its solutions are approximations of analytical solutions. A measure of the validity of these approximations is the norm $\|P^u(u_1, v_1) - P^s(u_2, v_2)\|$. One should accept only the approximate solutions for which this norm is smaller than a predetermined value.

Here, we proceeded as follows:

1. Initial values for parameters (ϵ, A) were chosen. Recall that ϵ should belong to the interval $[-1, 1]$, while parameter A belongs to the interval $[\frac{-2+\sqrt{2}}{4}, 0)$, to ensure that all eigenvalues of the fixed point at the origin are real.
2. For these parameter values, we solved system (12) for the coefficients of the (un)stable manifold. It was found that the lowest bound for the error $\|P^u(u_1, v_1) - P^s(u_2, v_2)\|$ was achieved when we computed terms up to order 80. Terms of higher order did not improve the error of our calculations.
3. We numerically solved equation (13). The solutions, with respect to unknowns u_1, v_1, u_2, v_2 , should satisfy $\|P^u(u_1, v_1) - P^s(u_2, v_2)\| < 10^{-10}$. Numerical solutions which did not fulfil this criterion were rejected.
4. If equation (13) had a solution fulfilling the criterion above, we concluded that an orbit homoclinic to the origin existed. If no such solution was found, the existence of a homoclinic orbit could not be established.
5. We then proceeded to other values of parameters (ϵ, A) .

The procedure described above permits us to draw the following:

Main numerical result: For mapping (8), orbits homoclinic to the origin exist for all $\epsilon \in (0, 1]$, $A \in [-0.145, -0.115]$.

A few observations are in order here.

First, for $\epsilon \in [-1, 0)$ no homoclinics were found. This is in accordance with the two-dimensional case, where the fixed point at the origin was stable if, and only if, $\epsilon > 0$.

Second, for positive values of ϵ , numerical solutions of equation (13) were found, even for values of A not belonging in $[-0.145, -0.115]$. The error bound at these solutions was, however, greater than 10^{-10} and they were therefore rejected.

Third, the error bound for the numerical solutions that we accepted was lower for values of ϵ closer to 0. The error bound was increasing, for $\epsilon \rightarrow 1$. Concerning parameter A , the error bound was found to be minimal in the middle of interval $[-0.145, -0.115]$.

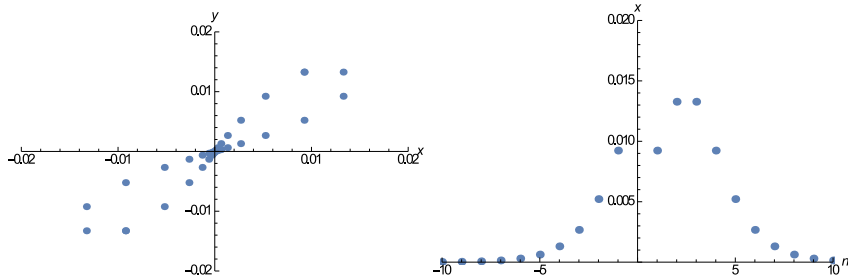


Figure 2: Left panel: the projection, on the $x - y$ plane of a pair of symmetric homoclinic orbits for mapping (8). Their calculation is presented in the example below. Right panel: the projection of a homoclinic orbit on the x -axis: it corresponds to a steady state soliton of equation (5).

We should note here that the numerical result presented above implies that equation (5) possesses steady-state solitons for $\epsilon > 0$ and $A \in [-0.145, -0.115]$. One can, approximately, construct these solitons using the x coordinate of the homoclinics found here.

Illustrative example: Set $A = -0.125$, $\epsilon = 0.0004$ and use system (12) to compute P^u, P^s up to terms of order 80. Equation (13) possesses solution:

$$\begin{bmatrix} u'_1 \\ v'_1 \\ u'_2 \\ v'_2 \end{bmatrix} = \begin{bmatrix} -0.6774898840489101 \\ 0.1347239986358392 \\ 0.1347239986358898 \\ 0.6774898840494726 \end{bmatrix},$$

which solution corresponds to the homoclinic point:

$$P^u(u'_1, v'_1) = P^s(u'_2, v'_2) = \begin{bmatrix} 9.23324715725 \cdot 10^{-3} \\ 1.32738452775 \cdot 10^{-2} \\ 1.32738452775 \cdot 10^{-2} \\ 9.23324715725 \cdot 10^{-3} \end{bmatrix}.$$

The errors involved in these calculations are found to be of order 10^{-13} .

In figure 2, left, the projection on the $x - y$ plane of the orbit of $P^u(u'_1, v'_1)$ is shown, along with its symmetric orbit. They converge to the origin for both positive and negative iteration. In the same figure, right, the x -coordinate of the orbit is shown. It corresponds to a steady-state soliton of equation (5).

Next, we wish to verify that the homoclinic points located here are transverse.

3.3 Transversality of homoclinic points

Let us consider a point $p \in W^u(O) \cap W^s(O)$. The intersection of $W^u(O)$, $W^s(O)$ is transversal at p , if $T_p W^u(O) \oplus T_p W^s(O) \simeq \mathbb{R}^4$. Since the invariant manifolds of the origin can be represented in parametric form S^u, S^s , as we saw above, the transversality condition can be expressed as:

$$\det \begin{bmatrix} \frac{\partial}{\partial u_1} S^u(u_1, v_1) \\ \frac{\partial}{\partial v_1} S^u(u_1, v_1) \\ \frac{\partial}{\partial u_2} S^s(u_2, v_2) \\ \frac{\partial}{\partial v_2} S^s(u_2, v_2) \end{bmatrix} \neq 0, \quad (14)$$

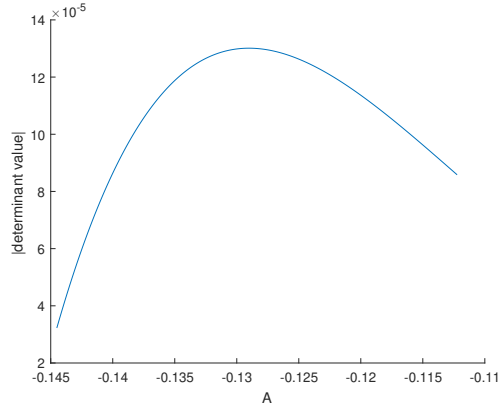


Figure 3: The value of the determinant (14), as a function of parameter A , for $\epsilon = 0.0002$. It is non-zero, for every value of A , implying the transverse intersection of the invariant manifolds of the origin.

where the determinant is evaluated at (u_1, v_1, u_2, v_2) corresponding to the point p , i.e. $S^u(u_1, v_1) = S^s(u_2, v_2) = p$.

Here, we use the expansions P^s , P^u obtained above, and compute, for $A \in [-0.145, -0.115]$ and $\epsilon \in (0, 1]$, the determinant appearing in the left-hand side of equation (14) at the approximate solutions calculated in the previous section. We found that parameter A has a strong influence on the value of the determinant, while the influence of parameter ϵ is indeed negligible.

In figure (3) we present the case where $\epsilon = 0.0002$. The value of the determinant is found to be non-zero, implying the transverse intersection of the invariant manifolds of the origin, for every value of $A \in [-0.145, -0.115]$.

To further study the effect parameter A has on the transversality of the intersection points, we computed the function which best fits the graph in figure (3). This function was found to be:

$$T(A) = 80.64A^4 + 33.74A^3 + 5.272A^2 + 0.3682A + 0.009737.$$

This function vanishes at points $A = -0.146292$ and $A = -0.0891431$, implying that homoclinic points exist even when A does not belong in the interval $[-0.145, -0.115]$ found above. This is probable due to the error bound used in our calculations: less strict error bounds would enlarge the existence interval of solutions for equation (13).

Indeed, by relaxing condition $\|P^u(u_1, v_1) - P^s(u_2, v_2)\| < 10^{-10}$ and allowing even bigger errors, we were able to locate homoclinic points for every $\epsilon > 0$, $A \in [\frac{-2+\sqrt{2}}{4}, 0)$, which we chose not to present here.

4 Conclusions

We studied a discrete NLS equation, with non-nearest neighbour interactions. This equation depends on two parameters, called ϵ and A . The equation, for $A = 0$, gives rise to a volume-preserving diffeomorphism of the plane, the behaviour of which turns out to be quite simple. For $A \neq 0$, however, seeking steady-state solutions of this equation, we get a four-dimensional diffeomorphism, the dynamical behaviour of which we analysed. We found that, for positive values of ϵ and for A belonging in an interval of the negative semi-axis, this mapping possesses orbits homoclinic to

the origin. Each such orbit corresponds to a steady-state discrete soliton of our discrete NLS-equation. Our techniques permit one not only to argue about the existence of these solitons but to also construct them, with great accuracy.

References

- [1] Ablowitz M J and Ladik J F, “Nonlinear differential-difference equations and Fourier analysis”, *J. Math. Phys.*, 17, 1011–1018, 1976.
- [2] Wu W P, Schrieffer J R and Heeger A J, Soliton excitations in polyacetylene, *Phys. Rev. B*, 22, 2099–2111, 1980.
- [3] Simó C, “Stability of degenerate fixed points of analytic area preserving mappings”, *Astérisque*, 98-99, 184-194, 1982.
- [4] Eilbeck J C, Lomsdahl P S and Scott A C, “The discrete self-trapping equation”, *Physica D*, 16, 318–338, 1985.
- [5] Kuznetsov E A, Rubenchik A M, Zakharov V E, “Soliton stability in plasmas and hydrodynamics”, *Phys. Rep.*, 142, 103, 1986.
- [6] Rasmussen J J, Rypdal K, “Blow-up in Nonlinear Schroedinger Equations-I A General Review”, *Phys. Scripta*, 33, 481, 1986.
- [7] Salerno M, “Quantum deformations of the discrete nonlinear Schrödinger equation”, *Phys. Rev. A*, 46, 6856–6859, 1992.
- [8] Ustinov A V, Doderer T, Vernik I V, Pedersen N F, Huebener R P and Oboznov V A, “Experiments with solitons in annular Josephson junctions”, *Physica D*, 68, 41–44, 1994.
- [9] Aceves A B, Luther G G, De Angelis C, Rubenchik A M and Turitsyn S K, “Energy localization in nonlinear fiber arrays: collapse-effect compressor”, *Phys. Rev. Lett.*, 75, 73–76, 1995.
- [10] Aubry S, “Breathers in nonlinear lattices: existence, linear stability and quantization”, *Physica D*, 103, 201–250, 1997.
- [11] Karpman V I, Shagalov A G, “Solitons and their stability in high dispersive systems. I. Fourth-order nonlinear Schrödinger-type equations with power-law nonlinearities”, *Phys. Lett. A*, 228, (59), 1997.
- [12] Lomelí H E and Meiss J D, “Quadratic volume preserving maps”, *Nonlinearity*, 11(3), 557-574, 1998.
- [13] Eisenberg H, Silberberg Y, Morandotti R, Boyd A and Aitchison J, “Discrete spatial optical solitons in waveguide arrays”, *Phys. Rev. Lett.*, 81, 3383–3386, 1998.
- [14] Lenz G, Talanina I and Martijn de Sterke, “Bloch oscillations in an array of curved optical waveguides”, *Phys. Rev. Lett.*, 83, 963–966, 1999.
- [15] Sterling D, Dullin H R and Meiss J D, “Homoclinic bifurcations for the Hénon map”, *Physica D*, 134, 153–184, 1999.
- [16] Flach S and Kladko K, “Moving discrete breathers?”, *Physica D*, 127, 61–72, 1999.

- [17] Dullin H R, Meiss J D, “Generalized Hénon maps: the cubic diffeomorphisms of the plane”, *Physica D*, 143 (1-4), 262-289, 2000.
- [18] Kevrekidis P G, Rasmussen K O, and Bishop A R, “The discrete nonlinear Schrödinger equation: a survey of recent results”, *Int. J. Mod. Phys. B*, 15, 2833–2900, 2001.
- [19] Shilnikov LP, Shilnikov A, Turaev D, Chua L, “Methods of Qualitative Theory in Nonlinear Dynamics”, *World Scientific*, 2001.
- [20] Fibich G, Ilan B, Papanicolaou G, “Self-focusing with fourth order dispersion”, *SIAM J. Appl. Math.*, 62, 4, 1437-1462, 2002.
- [21] Ablowitz M J, Musslimani Z H and Biondini G, “Methods For Discrete Solitons in Nonlinear Lattices”, *Phys. Rev. E*, 65, 026602, 2002.
- [22] Aigner A A, Champneys A R and Rothos V M, “A new barrier to the existence of moving kinks in Frenkel–Kontorova lattices”, *Physica D*, 186, 148–170, 2003.
- [23] Christodoulides D N, Lederer F and Silberberg Y, “Discretizing light behaviour in linear and nonlinear waveguide lattices”, *Nature*, 424, 817–823, 2003.
- [24] Fleischer J W, Carmon T, Segev M, Efremidis N K and Christodoulides D N, “Observation of Discrete Solitons in Optically Induced Real Time Waveguide Arrays”, *Phys. Rev. Lett.*, 90, 2003.
- [25] Li M C, Malkin M, “Bounded nonwondering sets for polynomial mappings”, *J.Dyn.Control Systems*, 10(3), 377-389, 2004.
- [26] Gonchenko S V, Ovsyannikov I I, Simó C, Turaev D, “Three dimensional Hénon–like maps and wild Lorenz–like attractors”, *Int.J.Bif.Chaos*, 15, 3493–3508, 2005.
- [27] Albiez M, Gati R, Fölling J, Hunsmann S, Cristiani M, and Oberthaler M K, “Direct Observation of Tunneling and Nonlinear Self-Trapping in a Single Bosonic Josephson Junction”, *Phys. Rev. Lett.* 95, 010402, 2005.
- [28] Basu S, Pollak R and Roy M-F, “Algorithms in Real Algebraic Geometry”, *Springer*, 2006.
- [29] Gonchenko S V, Meiss J D and Ovsannikov I I, “Chaotic Dynamics of three–dimensional Hénon maps that originate from a homoclinic bifurcation”, *Regul.Chaotic Dyn.*, 11(2), 191-212, 2006.
- [30] Gonchenko S, Li MC and Malkin M, “Generalized Hénon maps and Smale horseshoes of new types”, *Int.J.Bif.Chaos*, 18(10), 3029-3052, 2008.
- [31] Zhang X, “Hyperbolic invariant sets of the real generalized Hénon maps”, *Chaos Solitons and Fractals*, 43, 31-41, 2010.
- [32] Mireles–James J D, Lomel H, “Computation of heteroclinic arcs with application to the volume preserving Hénon family”, *SIAM J.App.Dyn.Sys.*, 9(3), 919–953, 2010.
- [33] Mireles–James J D, “Quadratic volume–preserving maps: (un)stable manifolds, hyperbolic dynamics, and vortex–bubble bifurcations”, *J.Nonlinear Sci.*, 23, 585–615, 2013.
- [34] Mireles–James J D, Mischaikow K, “Rigorous a posteriori computation of (un)stable manifolds and connecting orbits for analytic maps”, *SIAM J.Apl.Dyn.Sys.*, 12(2), 957–1006, 2013.
- [35] Haro À, Canadell M, Figueras J, Luque A, Mondelo J, “The Parameterization Method for Invariant Manifolds: From Rigorous Results to Effective Computations”, *Springer International Publishing*, 2016.

- [36] Gonchenko A S, Gonchenko S V, “Variety of strange pseudohyperbolic attractors in three-dimensional generalized Hénon maps”, *Phys. D*, 337, 43–57, 2016.
- [37] Anastassiou S, Bountis T, Bäcker A, “Homoclinic Points of 2-D and 4-D Maps via the Parametrization Method”, *Nonlinearity*, 30, 3799-3820, 2017.
- [38] Gonzalez J L, Mireles–James J D, “High–order parameterization of stable/unstable manifolds for long periodic orbits of maps”, *SIAM J. Appl.Dyn.Sys.*, 16(3), 1748–1795, 2017.
- [39] Capiński M J, Mireles–James J D, “Validated computation of heteroclinic sets”, *SIAM J.App.Dyn.Sys.*, 16(1), 375–409, 2017.
- [40] Anastassiou S, Bountis T, Bäcker A, “Recent results on the dynamics of higher dimensional Hénon maps”, *Reg.Chaot.Dynamics*, 23(2), 161-177, 2018.
- [41] Adams R, Mireles–James J D, “Validated numerics for continuation and bifurcation of connecting orbits of maps”, *Qual.Th.Dyn.Syst.*, 18, 107–137, 2019.
- [42] Anastassiou S, “Complicated behaviour in cubic Hénon maps”, *Theor.Math.Physics*, 207(2), 572-578, 2021.